

High Reliability and Luminance of Color Wheel by Novel Phosphor-in-Inorganic Silicone

CHUN-NIEN LIU,¹ HSING-KUN SHIH,¹ YI-CHIAN CHEN,² YUN-HUEI CHEN,³
WEI-CHIH CHENG,^{3,*} AND WOOD-HI CHENG³

¹Department of Electrical Engineering, National Chun Hsing University, Taichung, 402, Taiwan

²Department of Occupational Safety and Hygiene, Fooyin University, Kaohsiung, 831, Taiwan

³Graduate Institute of Optoelectronic Engineering, National Chun Hsing University, Taichung, 402, Taiwan

*Weichih0428@gmail.com

Abstract: A high reliability and luminance of color wheel in laser light engine (LLE) employing novel phosphor-in-inorganic silicone (PiIS) fabricated at low temperature of 180°C for laser projector applications is presented and demonstrated for the first time. Yellow ($\text{Y}_3\text{Al}_5\text{O}_{12}:\text{Ce}^{3+}$) and green ($\text{Lu}_3\text{Al}_5\text{O}_{12}:\text{Ce}^{3+}$) phosphors were uniformly mixed by inorganic silicone, organic silicone, and glass to fabricate as a phosphor color wheel. The PiIS based color wheels showed better thermal stability than the phosphor-in-organic silicone (PiOS) about 3-7 times less lumen loss and 7-8 times less chromaticity shift under accelerated aging at 350°C for 1008 hours. The advantage of the PiIS fabricated at a low temperature of 180°C enabled achievement of excellent thermal performance, which was similar to the phosphor-in-glass (PiG) fabricated at a high temperature of 680°C. The good thermal stability of the PiIS can be attributed to the high glass melting temperature up to 510°C. Low temperature fabrication, excellent optical performance, and high reliability of the proposed PiIS based color wheels benefit as promising candidates to replace the current PiOS or PiG based color wheels in the LLE modules for the next-generation laser projector applications.

© 2023 Optica Publishing Group under the terms of the Optica Open Access Publishing Agreement

1. Introduction

The projection displays usually required strong luminance on the spatial and angular to extend the beam in their light engines [1]. The laser-based projection system provides brighter light and efficiency for use in high power illuminating applications within the operating temperature of 350°C [2]. A common type of phosphor-converted color wheel consists of phosphor-doped silicone material because of its low cost and easy fabrication. However, the poor thermal stability of an organic silicone-based color wheel is due to the lower silicone transition temperature of 150°C. The high heat flux radiating from the high-power laser operation would make the organic silicone-based color wheel become etiolation, which could affect the optical performance of color wheel modules, such as luminous efficiency and chromaticity during usage [3]. Therefore, a novel carrier material of color wheels which has high power operation and absolute reliability for use in laser projector application is required.

Recently, the laser light engines (LLEs) based color phosphor-converted layers have been fabricated using organic silicone [4], glass [5-7], ceramic [8-10], and single crystal materials [11-12]. Table 1 lists the performance comparison of the fabrication temperature, thermal stability, advantages, and disadvantages of the phosphor-in-organic silicone (PiOS), phosphor-in-glass (PiG), phosphor-in-ceramic (PiC), phosphor-in-single crystal (PiSC), and phosphor-in-inorganic silicone (PiIS). The fabrication temperatures of the PiC and PiSC were over 1200°C and 1500°C, respectively. These high-temperature fabrications were difficult to be applied to the commercial production. In previous reports, the PiG showed better thermal stability than the PiOS of color conversion layers [13]. However, the PiG with lower conversion efficiency was due to the glass (SiO_2) and phosphor ($\text{Ce}^{3+}:\text{YAG}$) inter-diffusion at the

47 fabricated temperature of 700°C [14]. In order to achieve high reliability and luminance of high-
 48 quality color wheel, it is essential to develop a novel PiIS to combine high emission, strong
 49 thermal stability, and low fabricated temperature.

50 **Table 1. Comparison of phosphor-in organic silicone, glass, ceramic, single crystal, and inorganic silicone.**

	Fabrication temperature	Thermal stability	Advantages	Disadvantages
Phosphor-in-organic silicone (PiOS) [4]	~150°C	Poor	Better conversion efficiency Low-cost material	Poor thermal stability
Phosphor-in-glass (PiG) [5-7]	~700°C	Good	Better thermal stability	Lower conversion efficiency High-cost material
Phosphor-in-ceramic (PiC) [8-10]	>1200°C	Good	Better conversion efficiency	Higher fabrication temperature High-cost material
Phosphor-in-single-crystal (PiSC) [11,12]	>1500°C	Good	Better conversion efficiency	Higher fabrication temperature High-cost material
Phosphor-in-inorganic silicone (PiIS) (this study)	~180°C	Good	Better conversion efficiency and thermal stability	Medium-cost material

51
 52 In this study, a new scheme of high-reliable PiIS-based color wheel in the LLE for high-
 53 power laser operation and long-time laser operation is experimentally presented and
 54 demonstrated. The color temperatures of the yellow and green PiIS are controlled between
 55 4400K±100K, and 6300K±100K, respectively. We investigated the comparison of the optical
 56 performance for the PiIS- with the PiOS- and PiG-based color wheels and then conducted
 57 reliability tests at 150°C, 250°C and 350°C high temperature accelerated aging experiments for
 58 1008 hours. The results show that the PiIS-based color wheel exhibited better thermal stability
 59 than the PiOS-based color wheel in lumen loss and chromaticity shifts. Furthermore, the
 60 luminous flux of the PiIS exhibited almost the same intensity with PiOS and higher than PiG.
 61 The advantage of the PiIS fabricated at low temperature of 180 °C enabled achievement of good
 62 thermal performance, which was similar to the PiG fabricated at high of 680°C. The unique
 63 PiIS-based color wheel with high power operation and absolute reliability is essentially critical
 64 to replace commercially available PiOS [4] or PiG [5-7], and hence to provide a next-generation
 65 LLE module for use in laser projector applications.

66 **2. Experimental methodology**

67 Three phosphor-converter layers of the PiIS, PiOS, and PiG were analyzed and experimentally
 68 measured. In these phosphor color wheels, yellow phosphors ($Y_3Al_5O_{12}:Ce^{3+}$) and green
 69 phosphors ($Lu_3Al_5O_{12}:Ce^{3+}$) were uniformly mixed by inorganic silicone, organic silicone, and
 70 glass to fabricate as a phosphor converter layer for use in color wheels. The experiment
 71 comparison of the thermal stability and optical characteristics for the PiIS-, PiOS-, and PiG-
 72 based color wheel was investigated.

73 **2.1 Fabrication of the phosphor-in-inorganic and organic silicone**

74 The synthesis and characterization of the PiIS was explored, as shown in Fig. 1. There are four
 75 steps of sol-gel, powdering and mixing, dip-coating and sintering. Firstly, we mixed A-glue
 76 (colloidal anhydrous silica) and B-glue (hardening agent) evenly to complete the inorganic
 77 silicone in mass proportion as 1:1, and then joined the different proportions of the yellow
 78 phosphor and the green phosphor. The concentrations of the yellow and green phosphors were
 79 77.5 wt% and 82.5 wt%, respectively. The volume of the glass substrate was $80 \times 88 \times 0.55$ -
 80 mm³, the pattern of the mask was a square of 20×20 -mm², the coating thickness was controlled
 81 at 0.13-mm, and the mesh number was 60 with 0.25-mm aperture size, as shown at Fig. 2(a).

Finally, all mixed inorganic silicones with glass substrate was eliminated moisture at 85°C for 30 minutes, and then sintered at 180°C for 100 minutes. The PiISs were slowly cooled to room temperature and the internal stress of PiIS was reduced during this process. Figure 2 (b) and (c) showed the PiIS samples. The PiOS of the phosphor concentration, sample size, and fabricated process were similar to the PiIS. The AB glue of PiOS was used and formed by epoxy resin (component A) and polyfunctional hardener (component B) to get crosslinked and cured. Figure 2(d) and (e) showed the PiOS samples.

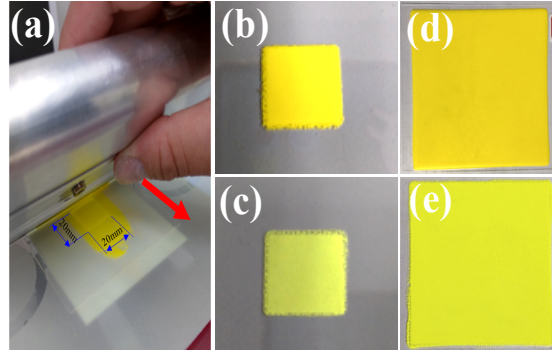
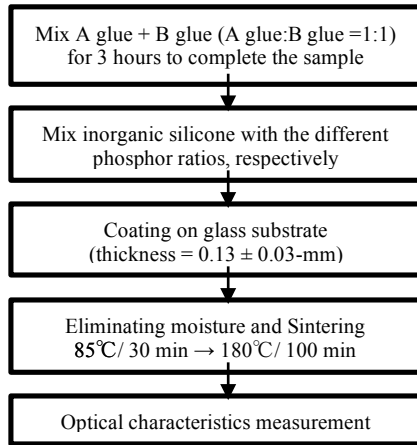


Fig. 1. Flow chart for phosphor-in-inorganic silicone. Fig. 2. (a) Screen printing process, (b) yellow PiIS, (c) green PiIS, (d) yellow PiOS, and (e) green PiOS.

2.2 Fabrication of the glass-based phosphor

The compositions of the glass matrix were B_2O_3 , Sb_2O_3 , SiO_2 , and Ta_2O_5 . These mixed raw materials were melted at 1080°C. After cooling, the glass matrix of the B_2O_3 - Sb_2O_3 - SiO_2 - Ta_2O_5 was ground into glass powders with a size of about 10- μm . Then, two different phosphors $Lu_3Al_5O_{12}:Ce^{3+}$ and $Y_3Al_5O_{12}:Ce^{3+}$ with a size of about 15 μm were uniformly spread out with different proportions and weight ratios of the 65wt% and 70wt% into the boron mother glass powder. These materials were uniformly mixed for 4 hours at 450 rpm by using a tubular vibration mixer. Then, the mixture powder was pressed uniaxially to form a precursor of the PiG and a precursor was sintered at temperature of 680°C for 30 minutes and annealed at 350°C for 120 minutes below the glass transition temperature. The thickness and diameter of the PiG was controlled to be 0.17-mm and 10-mm through a cutting and grinding process, respectively, as shown in Fig. 3. Table 2 lists the fabricated conditions of the PiIS, PiOS, and PiG samples.

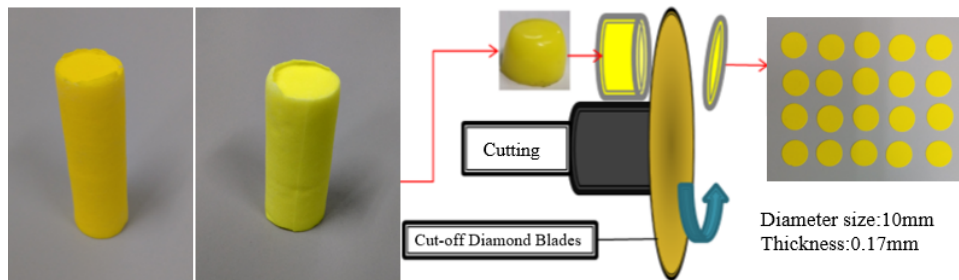


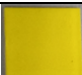





Fig. 3. Schematic diagram of PiG cutting and grinding process.

Table 2. The fabricated conditions of PiIS, PiOS, and PiG samples.

Sample index	Yellow ($\text{Y}_3\text{Al}_5\text{O}_{12}:\text{Ce}^{3+}$)		Green ($\text{Lu}_3\text{Al}_5\text{O}_{12}:\text{Ce}^{3+}$)	
Phosphor-in-inorganic silicone (PiIS)		Size: 20 x 20-mm ² Thickness: 0.13-mm Concentration: 77.5wt%		Size: 20 x 20-mm ² Thickness: 0.13-mm Concentration: 82.5wt%
Phosphor-in-organic silicone (PiOS) [4]		Size: 20 x 20-mm ² Thickness: 0.13-mm Concentration: 77.5wt%		Size: 20 x 20-mm ² Thickness: 0.13-mm Concentration: 82.5wt%
Phosphor-in-glass (PiG) [5-7]		Diameter size: 10-mm Thickness: 0.17-mm Concentration: 65wt%		Diameter size: 10-mm Thickness: 0.17-mm Concentration: 70wt%

3. Measurement and Results

Thermal stability was defined as the ability of the phosphor-in encapsulant to resist the action of heat and to maintain its optical properties, such as luminous flux, international commission on illumination (CIE), or correlated color temperature (CCT) at a limited temperature range [4-7, 15]. In order to realize the thermal analysis of the PiIS, PiOS, and PiG, the thermogravimetric analysis (TGA) was investigated. The mass of a sample was measured over time as the temperature changed. The analysis conditions included the reactant gas of 100 mL/min and the heating reactant rate of 5°C/min from 25°C to 950°C. This measurement provides information about physical phenomena, such as phase transitions, absorption, adsorption, and thermal decomposition [16]. Within a glass melting temperature, if the sample was thermally stable, there would be no observed mass change in the weight loss curve. Beyond the glass melting temperature the sample would begin to melt or degrade, which also showed that the heat flow curve was significantly decreased. In pervious study [15], the TGA result of PiG showed that the glass melting temperature is 519°C. Figure 4(a) showed that the first peak of the blue curve showed an endothermic peak at the around of 510°C, which was the glass melting temperature of PiIS. And the weight loss of the PiIS was a red curve and changed from 98% to 92%. Compared with PiIS and PiG, the PiOS of weight loss was changed from 98% to 63% at 320°C, as showed in Fig. 4 (b). The glass melting temperature of PiG and PiIS were higher than PiOS. It indicated that the PiG and PiIS could withstand higher temperatures and longer periods of operation, and demonstrated a good thermal stability.

In the scanning electron microscopy-energy dispersive X-ray spectrometry (SEM-EDS) experiment, the inorganic silicone phosphor material was analyzed. The detected C-, O- and Si-ions were verified that the PiIS samples were inorganic, as showed as in Fig. 5. The PiG samples were fabricated by glass matrix and phosphor, which were the inorganic. Compared with PiIS and PiG, the PiOS contained carbon-hydrogen or C-H bond, which were the organic [4].

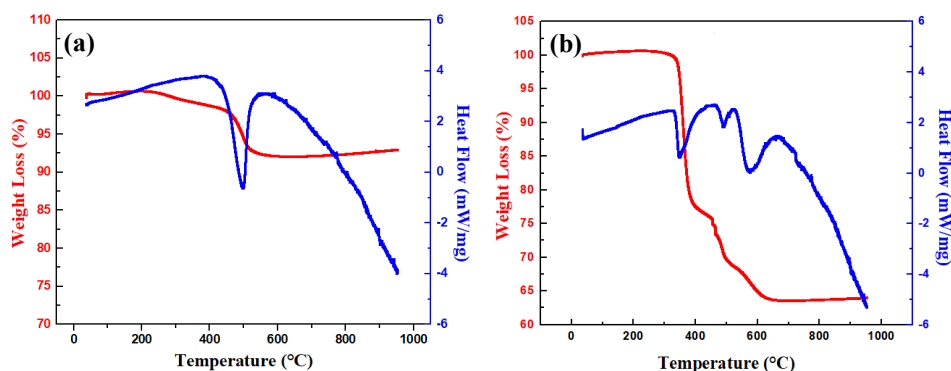


Fig. 4. The thermal analysis of (a) PiIS and (b) PiOS samples.

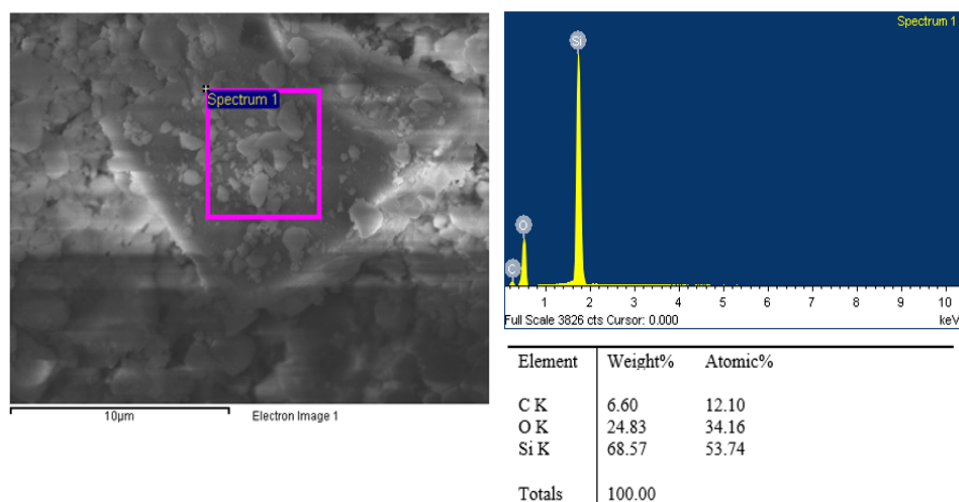


Fig. 5. The SEM-EDS result of PiIS sample.

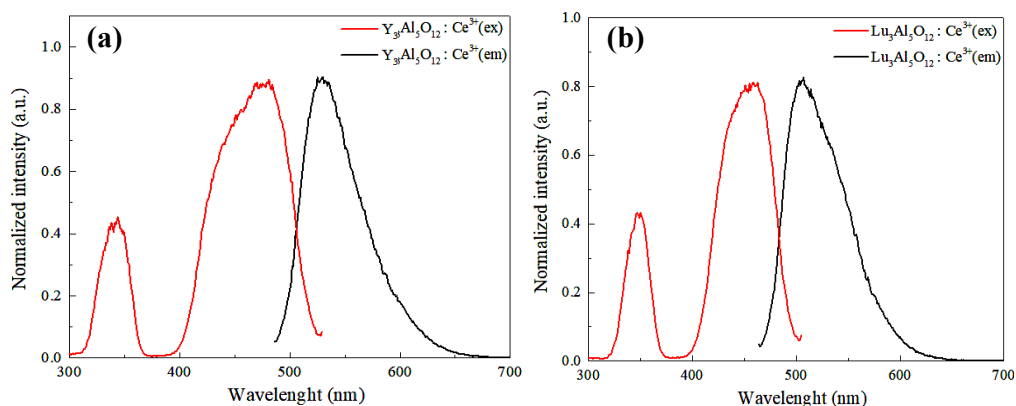


Fig. 6. The excitation and emission spectra of PiIS samples.

The light extraction efficiency of LLE referred to the amount of light that was emitted from light source and exited the color phosphor-converted layer, as a percentage of the total light generated within the LLE. This efficiency was an important factor to consider when designing LLE, as it affected the overall brightness and performance. Light extraction efficiency was influenced by a number of factors, minimizing Fresnel loss between phosphor/encapsulant interface was most important. Fresnel loss was proportional to the square of the difference between the refractive indices of the material interface and the cosine of the angle of incidence. Therefore, we used a prism coupler (Metricon 2010/M) with a 632nm He-Ne laser to calculate the refractive index of the PiOS, PiIS, PiG, and the phosphor. The He-Ne laser beam was directed through the prism into the testing sample and then reflected back out to the other side of the prism with a photo detector. However, the laser beam did not directly reflect back. We needed to control the rotary table to vary the incident angle of the laser, which would reflect back to the photo detector. The incident angle of laser could calculate the refractive index of testing sample from Snell's law [17]. The result showed that the refractive index of 1.40, 1.43, 1.41, and 1.80 were measured for the PiOS, PiIS, PiG, and phosphor, respectively. The index difference of the PiIS was lower than the PiOS and PiG. This indicated that light extraction efficiency of the PiIS was better than the PiOS and PiG

Photoluminescence (PL) excitation and emission spectra of the PiIS were collected at room temperature using a HITACHI U-4100 UV-VIS spectrometer and HITACHI F-4500 fluorescence spectrometer, respectively. The PL excitation (red curve) and emission (black curve) spectra of PiIS with two different phosphors ($\text{Y}_3\text{Al}_5\text{O}_{12}:\text{Ce}^{3+}$ and $\text{Lu}_3\text{Al}_5\text{O}_{12}:\text{Ce}^{3+}$) are shown in Fig. 6(a) and (b), respectively. The absorption band of $\text{Y}_3\text{Al}_5\text{O}_{12}:\text{Ce}^{3+}$ was between 400- to 520-nm and excited the emission from 500- to 620-nm with center wavelength of 534-nm. The absorption band of $\text{Lu}_3\text{Al}_5\text{O}_{12}:\text{Ce}^{3+}$ was between 400- to 500-nm and excited the emission from 480- to 600-nm with center wavelength of 513-nm.

The integrating sphere measurement system (Isuzu OPTICS ISM-360 series) was used to measure the light emission spectrum, chromaticity coordinates of the CIE, the CCT, and the luminous flux of PiIS, PiOS, and PiG samples. We used a 1.2- W_{opt} blue laser as light source of the wavelength of 442-nm. The operating voltage and current were 12V and 0.3mA, respectively. In the reflective measurement structure, a blue laser excitation light source needed to be attached to the integrating sphere, and an aluminum substrate was placed behind the different samples for measurement. Table 2 lists the results of optical performance of the PiIS, PiOS, and PiG samples. In order to compare with different materials between the PiIS, PiOS, and PiG, the color temperature of the yellow phosphors ($\text{Y}_3\text{Al}_5\text{O}_{12}:\text{Ce}^{3+}$) and the green phosphors ($\text{Lu}_3\text{Al}_5\text{O}_{12}$) were controlled within $4360\text{K}\pm 40\text{K}$ and $6300\text{K}\pm 40\text{K}$, respectively.

In the thermal stability study, the PiIS, PiOS, and PiG samples were tested at the operating laser power of 1.2 W_{opt} with aging temperature of 150°C, 250°C, and 350°C after 1008 hours. In this study, the batches of the PiIS, PiOS, and PiG samples of the yellow and green phosphors with high-power operation tests were investigated. The lumen loss and chromaticity shift were measured at each aging temperature to examine the degradation of three types of samples. Lumen loss referred to the reduction in the amount of luminous flux over operating time and was defined by %, $\text{LL} = (\text{Lm}_2 - \text{Lm}_1) / \text{Lm}_1$, where the Lm_1 and Lm_2 were the beginning and after operating time of luminous flux, respectively. Figure 7 showed the lumen loss as a function of test time of the PiIS, PiOS, and PiG samples of the yellow and green phosphor with high-power operation of 1.2 W_{opt} at aging temperature of 150°C, 250°C, and 350°C after 1008 hours. The lumen loss of the PiIS, PiOS, and PiG samples of the yellow and green phosphor were less than 1.89, 0.93, 5.99, 6.67, 1.89, and 1.33% at 350°C after 1008 hours, respectively. Figure 8 showed the CIE shift as a function of test time of the PiIS, PiOS, and PiG samples of the yellow and green phosphor with high-power operation of 1.2 W_{opt} at aging temperature of 150°C, 250°C, and 350°C after 1008 hours. The CIE shift of the PiIS, PiOS, and PiG samples of the yellow and green phosphor were about 4.0×10^{-3} , 4.0×10^{-3} , 40.5×10^{-3} , 30.9×10^{-3} , 5.4×10^{-3} , and 2.9×10^{-3} , at 350°C after 1008 hours, respectively, as shown in Table 3. In terms of appearance, the yellow and green phosphors of the PiIS indicated no cracks and PiOS indicated obvious cracks, respectively, as showed in Fig. 9(a) and (b). The inorganic material of the PiIS showed no other abnormality. Compared with the silicone-based samples of the yellow and green phosphors, the results indicated that the inorganic- and glass-based samples of the yellow and green phosphors shown lower lumen loss over test time. This indicated that the lumen loss of the silicone-based samples of the yellow and green phosphors were about 3.17 and 7.17 times higher than the inorganic- and glass -based samples of the yellow and green phosphors after 1008 hours at aging temperature of 350°C.

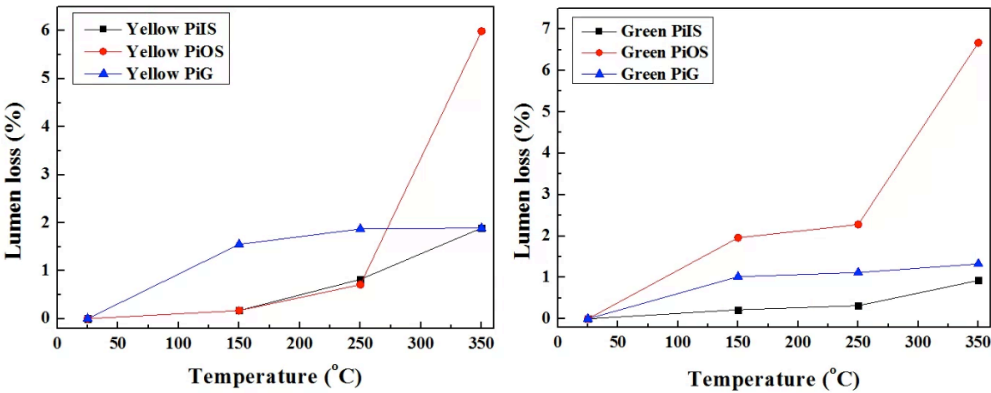
In general, the LLE module includes optical mirrors, diffuser glasses, blue laser diode, and color wheel. The color wheel is a key component for generating white light in the LLE. In this study, the PiIS-based color wheel can be divided into two segments based on the color of the doped phosphors, Y-segment (yellow) and G-segment (green), as shown in Fig. 10(a). A laser array was used as the light source to excite the color wheel to generate white light. The Y-segment and G-segment bonded on an aluminum substrate and then fixed on a micro-motor and then put into the LLE module for the laser projector, as shown in Fig. 10(b).

222

Table 3. Optical performances of the PiIS, PiOS, and PiG samples.

Sample index	Color	CIE (x, y)	CCT (K)	Luminous flux (lm)	Lumen loss (%)	CIE shift (10^{-3})
Phosphor-in-inorganic silicone (PiIS)	Yellow	(0.3863, 0.4632)	4338	40.57	1.89	4.0
	Green	(0.3013, 0.4699)	6287	42.95	0.93	4.0
Phosphor-in-inorganic silicone (PiOS) [4]	Yellow	(0.3810, 0.4495)	4391	40.03	5.99	40.5
	Green	(0.3004, 0.4685)	6313	42.80	6.67	30.9
Phosphor-in-glass (PiG) [5-7]	Yellow	(0.3803, 0.4408)	4370	36.18	1.89	5.4
	Green	(0.3010, 0.4588)	6328	37.20	1.33	2.9

223

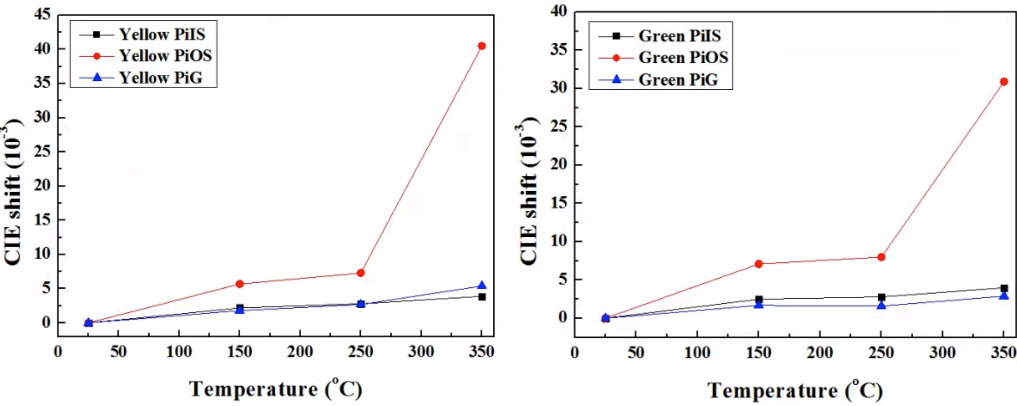


224

225

Fig. 7. Lumen loss of yellow and green phosphors time after 1008 hours of high temperature accelerated aging.

226

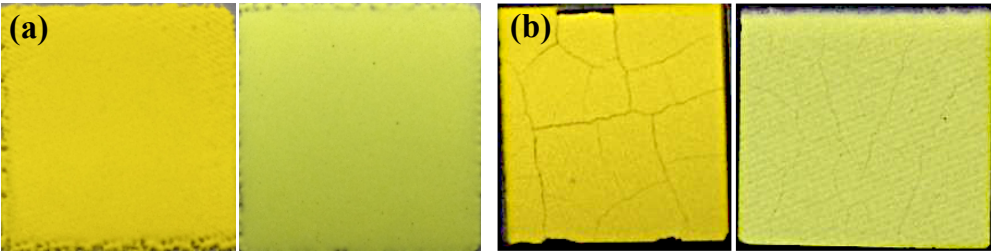


227

228

Fig. 8. CIE shift of yellow and green phosphors time after 1008 hours of high temperature accelerated aging.

229



230

231

232

Fig. 9. Appearance of yellow and green phosphor of (a) PiIS and (b) PiOS samples after 1008 hours at 350 °C.

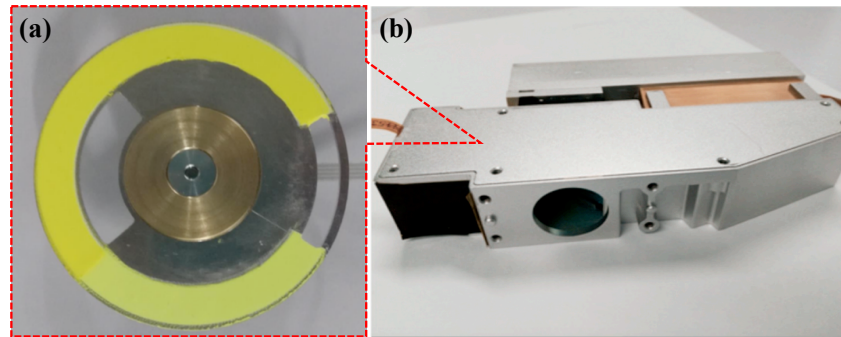


Fig. 10. (a) The PiIS-based color wheel with Y- and G-segment. (b) The LLE module with PiIS-based color wheel.

4. Discussion and conclusion

In summary, three phosphor-converter layers of the PiIS, PiOS, and PiG-based color wheels in the LLE for high-power laser operation and long-term reliability were experimentally investigated and their performance compared. The PiIS based color wheel showed better thermal stability than the PiOS based color wheel about 3-7 times less lumen loss and 7-8 times less chromaticity shift under accelerated aging at 350°C for 1008 hours. The advantages of the PiIS fabricated at low temperature of 180°C showed good thermal performance which was similar to the PiG fabricated a high temperature of 680°C. In this study, the proposed new scheme of high-reliable PiIS-based color wheel in the LLE exhibited low temperature fabrication of 180°C, better thermal stability, low-cost fabrication, and easy uniform phosphor coating with large-area processing. Therefore, this novel PiIS based color wheels benefit as promising candidates to replace the current PiOS or PiG based color wheels in the LLE modules for the next-generation laser projector applications.

Funding. National Science and Technology Council, Taiwan (NSTC) (111RB02, 111-2221-E-005-024-MY2, 111-2221-E-005-023-MY3, 110-2224-E-992-001); Ministry of Education (111RA077A, 110RA077A).

Disclosures. The authors declare that there are no conflicts of interest related to this article.

Data availability. Data underlying the results presented in this paper are not publicly available at this time but may be obtained from the authors upon reasonable request.

References

1. X. Huang, J. Liang, S. Rtimi, B. Devakumar, and Z. Zhang, "Ultra-high color rendering warm-white light-emitting diodes based on an efficient green-emitting garnet phosphor for solid-state lighting," *Chem. Eng. J.* **405**, 126950 (2021).
2. Y. Peng, Y. Mou, H. Wang, Y. Zhuo, H. Li, M. Chen, and X. Luo, "Stable and efficient all-inorganic color converter based on phosphor in tellurite glass for next-generation laser-excited white lighting," *J. Eur. Ceram. Soc.* **38**(16), 5525-5532 (2018).
3. Y. P. Chang, J. K. Chang, H. A. Chen, S. H. Chang, C. N. Liu, P. Han, and W. H. Cheng, "An advanced laser headlight module employing highly reliable glass phosphor," *Opt. Express* **27**(3), 1808-1815 (2019).
4. S. C. Allen, and A. J. Steckl, "A nearly ideal phosphor-converted white light-emitting diode," *Appl. Phys. Lett.* **92**, 143309 (2008).
5. C. C. Tsai, W. C. Cheng, J.K. Chang, L.Y. Chen, J. H. Chen, Y. C. Hsu, and W. H. Cheng, "Ultra-High Thermal-Stable Glass Phosphor Layer for Phosphor-Converted White Light-Emitting Diodes," *J. Display Technol.* **9**(6), 427-432 (2013).
6. H. Lee, S. Kim, J. Heo, and W. J. Chung, "Phosphor-in-glass with Nd-doped glass for a white LED with a wide color gamut," *Opt. Letters* **43**(4), 627-630 (2018).
7. H. K. Shih, C. N. Liu, W. C. Cheng, and W. H. Cheng, "High color rendering index of 94 in white LEDs employing novel CaAlSiN₃: Eu²⁺ and Lu₃Al₅O₁₂: Ce³⁺ co-doped phosphor-in-glass," *Opt. Express* **28**(19), 28218-28225 (2020).
8. S. M. Ohlberg, J. J. Hammel, and H. R. Golob, "Phenomenology of Noncrystalline Microphase Separation in Glass," *J. Am. Ceram. Soc.* **48**(4), 178-180 (1965).
9. M. Raukas, J. Kelso, Y. Zheng, K. Bergenek, D. Eisert, A. Linkov, and F. Jermann, "Ceramic Phosphors for Light Conversion in LEDs," *ECS J. Solid State Sci. Technol.* **2**(2), R3168-R3176 (2013).

276
277
278
279
280
281
282
283
284
285
286
287
288
289
290
291
292
293
294

10. H. Daicho, K. Enomoto, H. Sawa, S. Matsuishi, and H. Hosono, "Improved color uniformity in white light-emitting diodes using newly developed phosphors," *Opt. Express* **26**(19), 24784-24791 (2018).
11. M. Cantore, N. Pfaff, R. M. Farrell, J. S. Speck, S. Nakamura, and S. P. DenBaars, "High luminous flux from single crystal phosphor-converted laser-based white lighting system," *Opt. Express* **24**(2), A215-A221 (2016).
12. J. Xu, A. Thorseth, C. Xu, A. Krasnoshchoka, M. Rosendal, C. Dam-Hansen, B. Du, Y. Gong, O. B. Jensen, "Investigation of laser-induced luminescence saturation in a single-crystal YAG:Ce phosphor: Towards unique architecture, high saturation threshold, and high-brightness laser-driven white lighting," *J. Lumin.* **212**, 279-285 (2019).
13. Y. P. Chang, J. K. Chang, H. A. Chen, S. H. Chang, C. N. Liu, P. Han, and W. H. Cheng, "An advanced laser headlight module employing highly reliable glass phosphor," *Opt. Express* **27**(3), 1808-1815 (2019).
14. C. C. Tsai, W. C. Cheng, J. K. Chang, S. Y. Huang, J. S. Liou, G. H. Chen, Y. C. Huang, J. S. Wang, and W. H. Cheng, "Thermal-Stability Comparison of Glass- and Silicone-Based High-Power Phosphor-Converted White-Light-Emitting Diodes Under Thermal Aging," *IEEE Trans. Device Mat. Rel.* **14**(1), 4-8 (2014).
15. J. M. An, X. Zhao, D. S. Li, Y. J. Zhang, F. Fei, E. Y. B. Pun, and H. Lin, "New insights into phosphorescence properties of LuAGG: Long afterglow phosphor-in-glass for optical data storage," *Ceram. Int.*, **47**(3), 3185-3194 (2021).
16. A. W. Coats, and J. P. Redfern, "Thermogravimetric analysis. A review," *Analyst*, **88**(1053), 906-924 (1963).
17. R. Ulrich, and R. Torge, "Measurement of Thin Film Parameters with a Prism Coupler," *Appl. Opt.*, **12**(12), 2901-2908 (1973).